THE JOURNAL OF VISUALIZATION AND COMPUTER ANIMATION
J. Visual. Comput. Animat. 2000; **11**: 185–195

Illumination and acceleration in the visualization of special relativity: a comment on fast rendering of relativistic objects

By Daniel Weiskopf, Ute Kraus and Hanns Ruder*

We address the issue of illumination and acceleration in special relativistic visualization. Betts (J. Visual. Comput. Animat. 1998; 9: 17–31) presents an incorrect derivation of the transformation of the Rayleigh–Jeans radiation, which we compare to the correct transformation of radiance in the framework of special relativity. His rendering algorithm can be modified to correctly account for the relativistic effects on illumination. Furthermore, we show how acceleration can be included in special relativistic visualization by calculating the trajectory of accelerating objects, which is a prerequisite for a physically based camera model. Therefore interaction and animation in special relativistic visualization are possible. Copyright © 2000 John Wiley & Sons, Ltd.

Received: 20 August 1999; Revised: 14 January 2000

KEY WORDS: special relativity; simulation; illumination; animation; acceleration

Introduction

This paper is a comment on a work by Betts[1] in which he describes techniques for fast special relativistic rendering. In addition to the visualization of the apparent geometry of fast-moving objects, he considers illumination in the context of special relativity. He proposes a simplified illumination model in which the illuminants emit only Rayleigh–Jeans radiation. Therefore he investigates the transformation properties of the Rayleigh–Jeans spectral distribution, which is the large-wavelength limit of the blackbody power spectrum.

We agree with most parts of his paper, but we would like to correct his derivation of the relativistic transformation of the Rayleigh–Jeans spectrum and add the missing transformation of the spectrum of the light reflected by the objects. We present the correct transformation of the wavelength-dependent radiance for a general energy distribution. Based on this information, we derive expressions for the transformation of the Rayleigh–Jeans spectrum and of a line spectrum. We show how the original rendering algorithm can be modified to incorporate the correct transformation, leading to physically based relativistic illumination.

Furthermore, we give a comment on acceleration in special relativity, a subject widely ignored in previous work on special relativistic visualization. Betts alleges that special relativity does not deal with acceleration. Conversely, we show how special relativity is capable of describing accelerating objects.

Previous Work

It is remarkable that the issue of visual perception in special relativity was ignored for a long time, or wrong interpretations were given. Apart from a previously disregarded article by Lampa[2] in 1924 about the invisibility of the Lorentz contraction, the first solutions to this problem were given by Penrose[3] and Terrell[4] in 1959. Later, this issue was addressed in more detail by Weisskopf,[5] Boas,[6] Scott and Viner[7] and Scott and van Driel.[8]

*Correspondence to: D. Weiskopf, Institute for Astronomy and Astrophysics, University of Tübingen, Auf der Morgenstelle 10, D-72076 Tübingen, Germany.
E-mail: weiskopf@tat.physik.uni-tuebingen.de

Hsiung and Dunn[9] are the first to use advanced visualization techniques for image shading of fast-moving objects. They propose an extension of normal three-dimensional ray tracing. Hsiung and co-workers[10,11] add the visualization of the Doppler effect. Hsiung *et al.*[12] and Gekelman *et al.*[13] describe a polygon rendering approach which is based on the apparent shapes of objects as seen by a relativistic observer. This visualization technique is similar to the one presented by Betts. Polygon rendering is used as a basis for a virtual environment for special relativity in our previous work,[14,15] where we also describe the acceleration of a relativistic observer. In Reference 16 we focus on the issue of physically correct illumination in special relativistic visualization.

Physical Basis

In this section we state some important facts from the special theory of relativity. For a detailed presentation of the theory we refer to References 17–20.

Without loss of generality let us consider two inertial frames of reference, S and S', with S' moving with velocity v along the z axis of S. The usual Lorentz transformation along the z axis connects frames S and S'.

In reference frame S, consider a light ray whose direction is described by spherical co-ordinates θ and ϕ as shown in Figure 1. The wavelength is λ. In frame S' the direction is described by θ' and ϕ' and the wavelength by λ'. These two representations are connected by the expressions[19,21] for the Doppler effect,

$$\lambda' = \lambda D \tag{1}$$

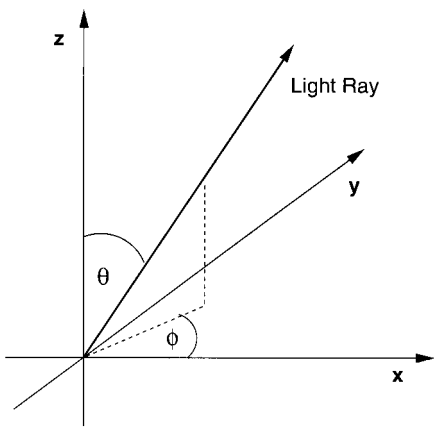

Figure 1. Light ray described by spherical co-ordinates.

and for the relativistic aberration of light,

$$\cos\theta' = \frac{\cos\theta - \beta}{1 - \beta\cos\theta} \tag{2}$$

$$\phi' = \phi \tag{3}$$

The Doppler factor D is defined as

$$D = \frac{1}{\gamma(1 - \beta\cos\theta)} = \gamma(1 + \beta\cos\theta')$$

where $\gamma = 1/\sqrt{1-\beta^2}$, $\beta = v/c$ and c is the speed of light. The Doppler effect causes a change in colour, whereas the aberration of light affects the apparent geometry of objects. The aberration of light is illustrated in Figure 2.

With equations (2) and (3) the transformation of solid angle is given by

$$\frac{\mathrm{d}\Omega'}{\mathrm{d}\Omega} = \frac{\sin\theta'}{\sin\theta}\frac{\mathrm{d}\theta'}{\mathrm{d}\theta} = \frac{\mathrm{d}(\cos\theta')}{\mathrm{d}(\cos\theta)} = \frac{1}{\gamma^2(1 - \beta\cos\theta)^2} = D^2 \tag{4}$$

Time dilation is another important phenomenon of special relativity and causes a change of time intervals at a fixed spatial position in S':

$$\mathrm{d}t' = \mathrm{d}t/\gamma \tag{5}$$

Radiance is the power per unit of foreshortened area emitted into a unit solid angle. In S the wavelength-dependent radiance is

$$L_\lambda(\lambda, \theta, \phi) = \frac{\mathrm{d}\Phi}{\mathrm{d}\lambda\ \mathrm{d}A_\perp \mathrm{d}\Omega} = \frac{\mathrm{d}\Phi}{\mathrm{d}\lambda\ \mathrm{d}A\ \mathrm{d}\Omega_\perp} \tag{6}$$

with the radiant flux Φ, the wavelength λ, the solid angle $\mathrm{d}\Omega$ and the area $\mathrm{d}A_\perp$, which is the area $\mathrm{d}A$ projected along the radiation direction (θ, ϕ). The radiant flux Φ is the radiant energy per unit time. The projected solid angle is $\mathrm{d}\Omega_\perp = \mathrm{d}\Omega\cos\theta$. By integrating over wavelengths, we obtain the radiance

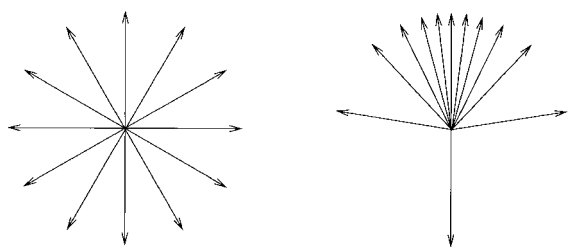

Figure 2. Aberration of light. The left figure shows some of the light rays emitted by a point-like isotropic light source in its rest frame. The right figure shows the same light rays with the source moving upwards at $\beta = 0.9$.

$$L(\theta,\phi)=\frac{\mathrm{d}\Phi}{\mathrm{d}A_{\perp}\mathrm{d}\Omega}=\frac{\mathrm{d}\Phi}{\mathrm{d}A\ \mathrm{d}\Omega_{\perp}}$$

Figure 3 illustrates the geometry of the quantities needed for the computation of radiance.

In S' the wavelength-dependent radiance can be obtained by

$$L'_{\lambda}(\lambda',\theta',\phi')=D^{-5}L_{\lambda}(\lambda,\theta,\phi) \tag{7}$$

The derivation of this equation can be found in our previous work.[16] The transformation of radiance increases the apparent brightness of objects ahead when the observer is approaching these objects at high velocity.

Illumination in Special Relativistic Rendering

Betts proposes a special scenario which simplifies the calculation of illumination in special relativistic visualization. The illuminants emit only Rayleigh–Jeans radiation and the reflectance properties of the objects are described by an extension of the usual RGB model.

Betts investigates the transformation of the 'intensity' of the Rayleigh–Jeans distribution from one inertial frame of reference to another. In the literature, the term 'intensity' is used for various quantities describing some kind of 'brightness'. In Reference 22, intensity is defined as the radiant power per unit solid angle and only makes sense as a measure of radiant energy leaving a point light source. Since Betts does not define 'intensity' and uses radiance in other parts of his paper, we will consider only radiance in the remaining parts of our paper. Moreover, radiance is the basic measure of 'brightness' in computer graphics because, in one inertial frame of reference, it does not vary with distance *in vacuo*.

Betts' Derivation of the Transformation of Rayleigh–Jeans Radiation

Betts investigates the transformation properties of the Rayleigh–Jeans radiation. However, his derivation of the transformation of wavelength-dependent radiance is not correct because of the following reasons.

The photon energy is not proportional to the inverse square of wavelength. The photon energy E and wavelength λ are correctly related by $E=hc/\lambda$, with h being the Planck constant.

It is not the case that the range of the original spectrum that is shifted to the visual region directly varies with wavelength—neither for relativistic nor for non-relativistic Doppler shifting. Based on the relativistic Doppler effect, we obtain the transformed infinitesimal wavelength interval $\mathrm{d}\lambda'=\mathrm{D}\ \mathrm{d}\lambda$ from equation (1). Since the Doppler factor D is independent of wavelength, finite wavelength intervals transform in the same way, i.e. $\Delta\lambda'=D\ \Delta\lambda$. Based on the non-relativistic Doppler effect, the transformed infinitesimal wavelength interval would be $\mathrm{d}\lambda'=(1+\beta\cos\theta')\mathrm{d}\lambda$. However, the difference between the relativistic and the non-relativistic Doppler effect cannot be neglected

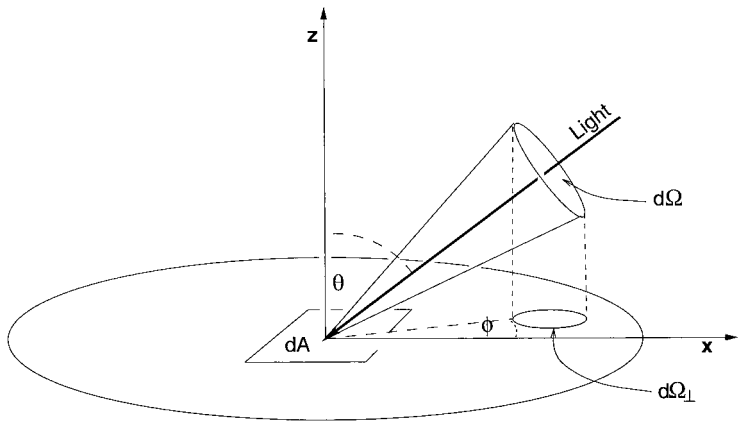

Figure 3. Geometry for calculation of radiance L. *The direction of the incoming light is given by* θ *and* ϕ. *The light is emitted from the solid angle* $\mathrm{d}\Omega$ *onto the area* dA.

at velocities as high as used in Betts' article. At $\beta = 0.99$, for example, the transformed wavelength in the relativistic case is approximately seven times larger than in the non-relativistic calculation.

Time dilation, i.e. the transformation of time intervals, is not considered in Betts' work. However, radiance depends on the time interval in which the photons are counted.

The transformation of solid angle is neglected by Betts. However, radiance depends on the solid angle from which photons are emitted. Owing to relativistic aberration, one obtains $d\Omega' = D^2\, d\Omega$ (see equation (4)).

Finally, Betts obtains the incorrect result that the wavelength-dependent radiance of the Rayleigh–Jeans radiation is independent of the frame of reference.

Correct Transformation of Rayleigh–Jeans Radiation

The wavelength-dependent radiance for the Rayleigh–Jeans radiation is

$$L_{\lambda,\mathrm{R\text{–}J}} = C\frac{1}{\lambda^4}$$

with $C = 2ckT$. T is the temperature and k is the Boltzmann constant. The Rayleigh–Jeans spectrum is the large-wavelength limit of the blackbody Planck spectrum.

Based on equation (7), we can calculate the transformed wavelength-dependent radiance for the Rayleigh–Jeans distribution:

$$\begin{aligned} L'_{\lambda,\mathrm{R\text{–}J}}(\lambda') &= D^{-5} L_{\lambda,\mathrm{R\text{–}J}}(\lambda) \\ &= D^{-5} L_{\lambda,\mathrm{R\text{–}J}}(\lambda'/D) = D^{-5} C D^4 \lambda'^{-4} \\ &= D^{-1} L_{\lambda,\mathrm{R\text{–}J}}(\lambda') = \frac{\lambda}{\lambda'} L_{\lambda,\mathrm{R\text{–}J}}(\lambda') \end{aligned} \tag{8}$$

Therefore the wavelength-dependent radiance of the Rayleigh–Jeans distribution is not independent of the frame of reference, but is transformed like the inverse of the wavelength of the photons. The transformed spectrum is still a Rayleigh–Jeans spectrum, but its value is scaled by a factor of D^{-1}.

The human eye, a camera or a detector has a wavelength-dependent efficiency. Therefore the perceived or measured wavelength-dependent radiance has to be weighted by a weighting function $w(\lambda)$. With the use of equation (8) the perceived radiance can be obtained by

$$\begin{aligned} L'_{\mathrm{perceived,R\text{–}J}} &= \int_{\mathrm{supp}(w)} w(\lambda') L'_{\lambda,\mathrm{R\text{–}J}}(\lambda')\, d\lambda' \\ &= D^{-1} \int_{\mathrm{supp}(w)} w(\lambda') L_{\lambda,\mathrm{R\text{–}J}}(\lambda')\, d\lambda' \\ &= D^{-1} \int_{\mathrm{supp}(w)} w(\lambda) L_{\lambda,\mathrm{R\text{–}J}}(\lambda)\, d\lambda \\ &= D^{-1} L_{\mathrm{perceived,R\text{–}J}} \end{aligned}$$

The support of the weighting function, $\mathrm{supp}(w)$, is a wavelength interval, e.g. the range of the visible wavelengths [380 nm, 780 nm]. For the human eye the standard luminous efficiency function $V(\lambda)$ is normally used as weighting function.[23,24] Note that the transformation of the radiance,

$$L'_{\mathrm{perceived,R\text{–}J}} = D^{-1} L_{\mathrm{perceived,R\text{–}J}} = \frac{\lambda}{\lambda'} L_{\mathrm{perceived,R\text{–}J}}$$

is valid for an arbitrary weighting function.

Modelling Colour

For an accurate computation of colour and illumination in special relativity, a large portion of the spectral energy distribution transferred between light sources, objects and the observer has to be considered. In order to simplify these calculations, Betts proposes an extension of the usual RGB colour model for the visualization of relativistic effects on colour. He uses either a triplet of ⟨r,g,b⟩ or a quintuplet of ⟨infrared,r,g,b,ultraviolet⟩. The RGB peaks are located at the wavelengths for the respective primaries. The infrared and ultraviolet peaks are located at arbitrary wavelengths outside the visual spectrum.

This approach can be generalized to a line spectrum consisting of an arbitrary, yet finite number of peaks. A single peak can be represented by a delta distribution δ (or 'delta function'). For an introduction to distributions we refer to References 25 and 26. The wavelength-dependent radiance can then be described by

$$L_{\lambda,\mathrm{line}}(\lambda,\theta,\phi) = \sum_{i=1}^{n} a_i(\theta,\phi)\,\delta(\lambda - \lambda_i) \tag{9}$$

where n is the number of peaks, λ_i is the wavelength for peak i and a_i is the weight of peak i.

In Betts' illumination model, only the Doppler shift of the wavelength of the line spectrum is considered, but the transformation of radiance is completely ignored. When calculating the RGB values from a

Doppler-shifted line spectrum, he neglects the wavelength-dependent efficiency of the human eye and uses a simple interpolation between the RGB primaries in the RGB colour vector space.

With the use of equation (7) and with the following property of a delta distribution,

$$\delta(ax) = \frac{1}{a}\delta(x)$$

the transformed wavelength-dependent radiance of the line spectrum is

$$L'_{\lambda,\text{line}}(\lambda', \theta', \phi') = D^{-4} \sum_{i=1}^{n} a_i(\theta, \phi)\delta(\lambda' - \lambda'_i) \qquad (10)$$

The transformed spectrum is still a line spectrum. The peaks are now located at the Doppler-shifted wavelengths $\lambda'_i = D\ \lambda_i$ and the weights of the peaks are scaled by D^{-4}.

The spectral energy distribution of the light reaching the camera has to be transformed to RGB values, which can be displayed on a monitor. In general, the RGB values are calculated by

$$R = \int L_\lambda(\lambda)\bar{r}(\lambda)\ d\lambda$$

$$G = \int L_\lambda(\lambda)\bar{g}(\lambda)\ d\lambda$$

$$B = \int L_\lambda(\lambda)\bar{b}(\lambda)\ d\lambda$$

where $\bar{r}(\lambda)$, $\bar{g}(\lambda)$ and $\bar{b}(\lambda)$ are the colour-matching functions for RGB.[24] For a line spectrum we obtain the RGB values perceived by the relativistic observer by

$$R = D^{-4} \sum_{i=1}^{n} a_i(\theta, \phi)\bar{r}(\lambda'_i) \qquad (11)$$

$$G = D^{-4} \sum_{i=1}^{n} a_i(\theta, \phi)\bar{g}(\lambda'_i) \qquad (12)$$

$$B = D^{-4} \sum_{i=1}^{n} a_i(\theta, \phi)\bar{b}(\lambda'_i) \qquad (13)$$

If the final RGB values lie outside the monitor gamut, they will be clamped to displayable values. More information about gamut mapping and the issue of correct colour reproduction can be found in References 27 and 28. A detailed presentation of colour calculations for computer graphics is given by Glassner.[29]

The transformation of a given colour to a spectral energy distribution is not unique, i.e. a colour corresponds to many different spectra. This effect is called metamerism. Betts uses a linear combination of delta distributions to solve this problem. Other basis functions have been proposed, such as box functions,[28,30] Fourier functions[22] and Gaussian functions.[31] The relativistic transformation of wavelength-dependent radiance can be applied to these basis functions in a similar way as above.

The Rendering Algorithm

The correct transformation of the wavelength-dependent radiance for the Rayleigh–Jeans distribution and the improved colour model can easily be incorporated into the rendering algorithm described by Betts. Only two modifications are needed.

First, for the initial shading of the objects the transformation of wavelength-dependent radiance has to be taken into account (cf. Betts' paper, point four of the initialization). Betts assumes a special situation in which the objects are moving at constant velocity and all light sources emit Rayleigh–Jeans radiation from infinite distance (i.e. directional light). With the relativistic transformation, equation (8), the wavelength-dependent radiance reaching the object and the local illumination model can be computed. This calculation can be done in a preprocessing step and does not impair performance during runtime.

Secondly, the calculation of the colour of each point has to be extended by the transformation of wavelength-dependent radiance (cf. Betts' paper, point two of the calculation for every frame). The Doppler factor is already determined in order to model colour shift. Therefore the transformation of the line spectrum reaching the observer and the final mapping of the transformed line spectrum to RGB values, equations (11)–(13), cause only minimal extra computational cost.

In the general situation with arbitrary spectral energy distributions of the illuminating light sources and with non-trivial material properties of the illuminated objects, the wavelength-dependent radiance has to be taken into account in all intermediate calculations. This could be implemented by using a point-sampled spectral energy distribution, or by using a general linear colour representation which consists of a finite number of orthonormal basis functions.[32] Whenever the frame of reference is changed, the transformation of wavelength and wavelength-

dependent radiance has to be considered according to equations (1) and (6). For final image synthesis, three tristimulus values RGB can be obtained from the wavelength-dependent radiance that reaches the eye point. Note that the spectral energy distribution has to be known over an extensive range so that the Doppler-shifted energy distribution can be determined for wavelengths in the visible range.

Results of Relativistic Rendering

Examples of special relativistic visualization can be found in Figures 4–7. Figure 4 illustrates the relativistic transformation of radiance for the Rayleigh–Jeans distribution. Here the relativistic transformation changes only the brightness but not the colour of the light. Figure 5 shows the same situation for the Planck distribution. Since the Rayleigh–Jeans distribution varies from the Planck distribution for small wavelengths, the main differences occur for the red-shifted, rightmost parts of the pictures.

Figure 6 illustrates the relativistic effects on a line spectrum. The image generation is based on the full spectral energy distribution reaching the eye point. The spectrum is peaked around the wavelengths 435, 545 and 700 nm for the blue, green and red primaries respectively. The various colours are modelled by adjusting the weights of the peaks. Figure 6(b) shows the visualization of the Doppler effect only, i.e. merely the wavelengths of the spectral energy distribution are transformed. In Figure 6(c) the transformation of wavelength-dependent radiance is included. A low velocity of only $\beta = 0.25$ is used in order to restrict the Doppler shifting of the small-band line spectrum to a reasonable range.

The difference between the visualization of the Doppler effect only and the visualization with a complete transformation of wavelength-dependent radiance dramatically increases at high velocities owing to the highly non-linear dependence of radiance on the Doppler factor. Figure 7 illustrates the relativistic effects for a scene which is illuminated by Planck radiation. Here the objects are colourless Lambertian reflectors. Figure 7(b) shows the blue shift due to the Doppler effect. In Figure 7(c), for the transformation of radiance to be displayed, the overall illumination has to be reduced to 1/1000th compared to that in the images in Figures 7(a) and 7(b). Owing to the transformation of radiance, the objects ahead are extremely bright. This is a most impressive example for the effects of the transformation of radiance.

All images were generated by the relativistic polygon-rendering program *Virtual Relativity*.[14,15]

Acceleration in Special Relativity

Acceleration in the visualization of special relativity is a subject widely neglected. For example, there is no reference to acceleration in References 9–11, 33 and 34. In our previous work[14,15] we describe the acceleration of an observer within a virtual environment for special relativity. The paper by Gekelman *et al.*[13] is the only other work known to us which addresses the issue

Figure 4. Visualization of the relativistic transformation of radiance for the Rayleigh–Jeans distribution with a temperature of T = *10,000 K. The left image shows a radiating sphere at rest. The other images show the same sphere moving from the left to the right with* $\beta = 0.9$.

Figure 5. Visualization of the relativistic transformation of radiance for the Planck distribution with a temperature of T = *10,000 K. The left image shows a radiating sphere at rest. The other images show the same sphere passing by with* $\beta = 0.9$.

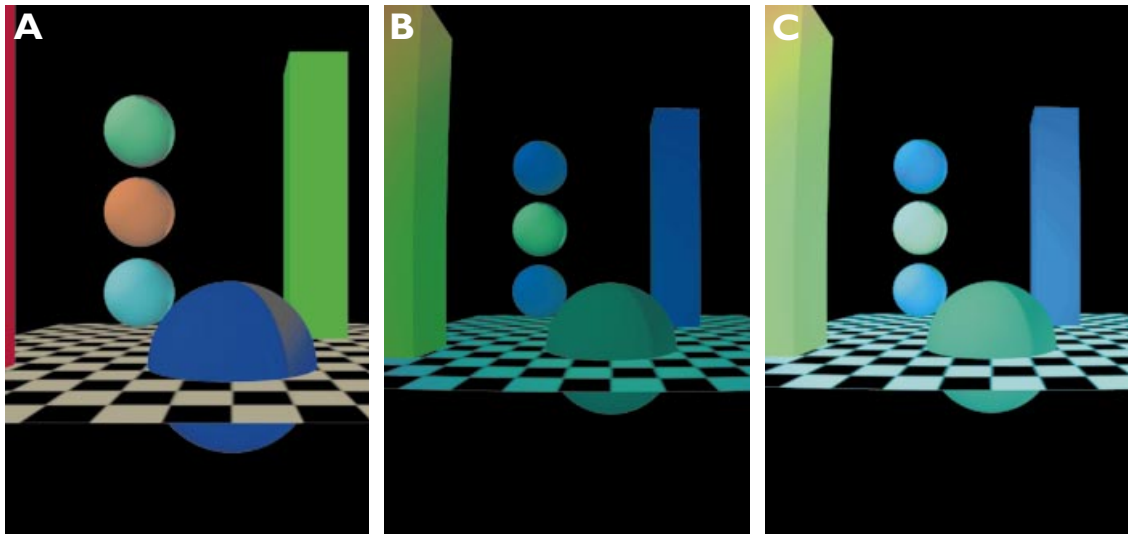

Figure 6. Visualization of the Doppler effect and the transformation of radiance for the original colour model. Image (a) shows a non-relativistic view on the test scene. Image (b) illustrates the Doppler effect. The viewer is moving with $\beta = 0.25$ into the test scene. The apparent geometry of the objects is changed according to the relativistic aberration of light, equations (2) and (3). Image (c) shows the same situation with the complete relativistic transformation of wavelength-dependent radiance being included.

of acceleration in special relativistic rendering. However, Gekelman *et al*. do not describe acceleration in detail.

Betts states that special relativity does not deal with accelerating objects and that acceleration is under the purview of general relativity. This is not the case.

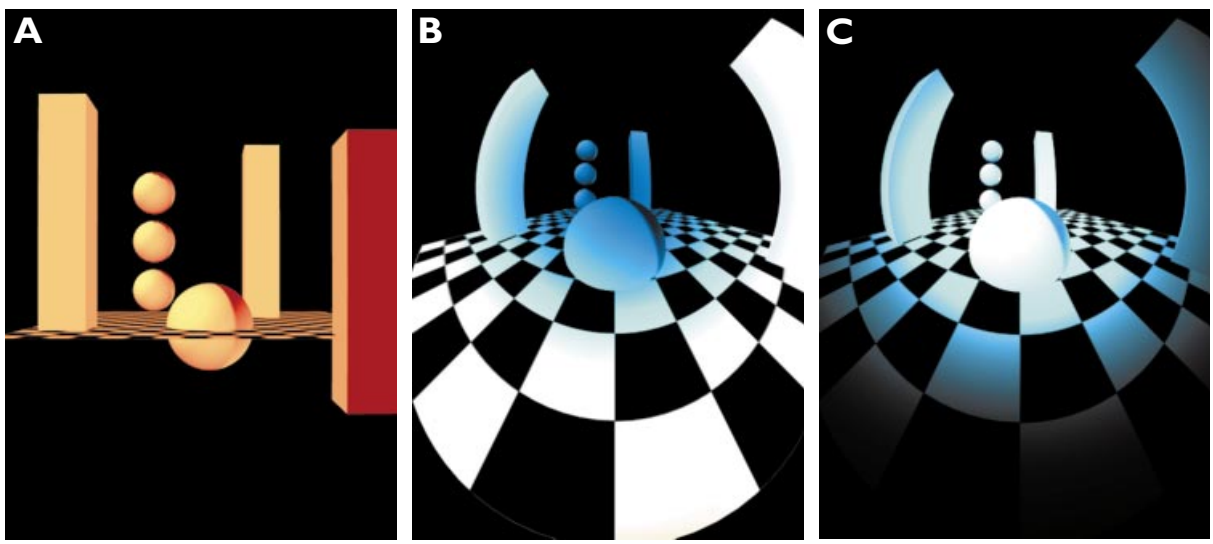

Figure 7. Visualization of the Doppler effect and the transformation of radiance for a scene which is illuminated by Planck radiation with a temperature of 2800 K. Image (a) shows a non-relativistic view on the test scene. Image (b) illustrates the Doppler effect. The viewer is moving with $\beta = 0.9$ into the test scene. The apparent geometry of the objects is changed according to the relativistic aberration of light. Image (c) shows the same situation with the complete relativistic transformation of wavelength-dependent radiance being included. Here the overall illumination is reduced to 1/1000th of that in (a) and (b).

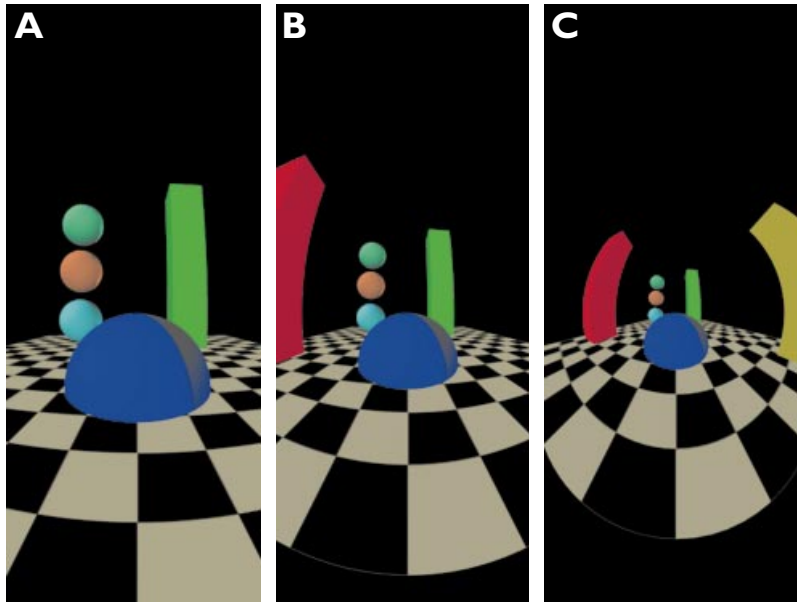

Figure 8. Visualization with an accelerating observer. The observer is rushing into the test scene shown in Figure 6(a). The velocities are $\beta =$ (a) 0.6, (b) 0.815 and (c) 0.956. The images show only the apparent geometry. The Doppler and searchlight effects are neglected.

Special relativity is perfectly capable of describing acceleration as long as gravitation is ignored. (Gravitation is the domain of general relativity.) The fact that the kinematics of particles in high-energy particle accelerators can be described by special relativity is only one piece of experimental evidence for this statement. In the storage ring HERA (Hadron–Electron Ring Accelerator) at DESY (http://www.desy.de), for example, electrons and positrons are accelerated up to an energy of 30 GeV, which yields a velocity of approximately $\beta = 0.99999999985$. The circular motion of these particles in the storage ring is caused by acceleration by electromagnetic fields. The calculation of this acceleration and of the collision experiments is based on special relativity and is in perfect agreement with the experiment.

Lorentz transformations are restricted to inertial frames of reference. However, a co-moving inertial frame can be found at every point in spacetime even for an accelerating object. This way, expressions known from inertial frames of reference can be used. The concept of co-moving frames of reference enables us to deal with acceleration in special relativity. In the Appendix the mathematical framework for the description of an accelerating point particle is presented.

Acceleration is a prerequisite for more advanced visualization techniques, including animation, navigation and user interaction.

One example is the implementation of a relativistic camera model which allows the user to navigate through a virtual environment.[14,15] Here the steering resembles flying in an aircraft or spaceship. The motion of the camera is controlled by the user, who provides information about the acceleration applied.

The computation of the trajectory of the camera and relativistic rendering are completely separate processes. In fact, relativistic rendering is not sensitive to acceleration. The production of a snapshot is only determined by the position, velocity and direction of motion of the observer and by the standard camera parameters. The rendered image is identical to the image seen by a co-moving observer. However, acceleration affects the motion of the camera and thus its position and speed. Although the generation of a single snapshot is not altered by acceleration, the appearance of a film sequence is heavily influenced by the changing velocity and position of the camera due to acceleration.

This effect is illustrated by the example in Figure 8. The observer is rushing into the scene with increasing speed. Here only the visualization of apparent geometry is used and the Doppler and searchlight effects are neglected. This way, the geometric effects of acceleration become much more apparent. Contrarily to everyday perception, the objects seem to move away from the observer although the observer is approaching the

objects at rising speed. This effect is caused by the increasing relativistic aberration of the incoming photons.

Future work could comprise more sophisticated applications of acceleration which include complex animation and motion of the objects. For example, the condition of a point particle might be dropped and the dynamics and internal forces of an extended object could be investigated.

Conclusion

We have presented the transformation of wavelength-dependent radiance from one inertial frame of reference to another. We have applied this transformation to the special cases of the Rayleigh–Jeans spectrum and a line spectrum. The original rendering algorithm needs only slight modifications to incorporate the transformation of radiance and a correct colour model, whereas rendering performance is not impaired. Therefore a fast and correct visualization of apparent geometry, colour and brightness in special relativity is possible.

Furthermore, we have shown how to treat acceleration within the realm of special relativity. Acceleration is an important part of the visualization of special relativity and enables us to consider more sophisticated elements of visualization, such as animation, navigation or user interaction.

ACKNOWLEDGEMENTS

We would like to thank the anonymous reviewers for very useful remarks. Special thanks are due to Bettina Salzer for proof-reading. This work was supported by the Deutsche Forschungsgemeinschaft (DFG) and is part of project D4 within Sonderforschungsbereich 382.

Appendix: Mathematical Description of Acceleration

In this appendix the mathematical background for the description of acceleration is presented. We restrict ourselves to point-like objects.

For a convenient description of accelerating objects the notion of spacetime and four-vectors has to be introduced. A detailed presentation can be found in References 17–20. The time co-ordinate t and the three spatial co-ordinates (x,y,z) can be combined to form the position four-vector

$$x^\mu = (ct, x, y, z) = \left(x^0, x^1, x^2, x^3\right), \quad \mu = 0, 1, 2, 3$$

The position four-vector describes a point in spacetime, i.e. an event in spacetime. A general four-vector is defined as a quantity whose four components are transformed by Lorentz transformation in the same way as the position coordinates (x^0,x^1,x^2,x^3).

The proper time τ is defined as the time measured by a co-moving clock and is thus independent of the frame of reference. Owing to time dilation, equation (5), the differential proper time is given by

$$\mathrm{d}\tau = \sqrt{1-\beta^2}\,\mathrm{d}t = \frac{\mathrm{d}t}{\gamma}$$

Classical quantities such as velocity and acceleration can be extended to corresponding four-vectors. The four-velocity is defined by

$$u^\mu = \frac{\mathrm{d}x^\mu}{\mathrm{d}\tau} \tag{14}$$

The four-acceleration of an object is given by

$$a^\mu = \frac{\mathrm{d}u^\mu}{\mathrm{d}\tau} \tag{15}$$

In a frame of reference in which the object is at rest at a respective point in space, the four-acceleration and the usual acceleration in three-dimensional space (a_x, a_y, a_z) are related by

$$a^\mu = \left(0, a_x, a_y, a_z\right) \tag{16}$$

When the object is accelerating, it is not sufficient to specify only a single inertial frame of reference, but a frame of reference for every point on the trajectory of the object. The Minkowski diagram in Figure 9 illustrates accelerated motion through spacetime and the co-moving frames of reference. The Minkowski diagram is a spacetime diagram without the co-ordinates y and z. Please note that the direction of the t axis of a co-moving frame is always tangential to the trajectory of the object.

Combining equations (14) and (15), one obtains the equations of motion,

$$\frac{\mathrm{d}^2x^\mu}{\mathrm{d}\tau^2} = a^\mu$$

This is a system of second order ordinary differential equations. For given initial values and given accelera-

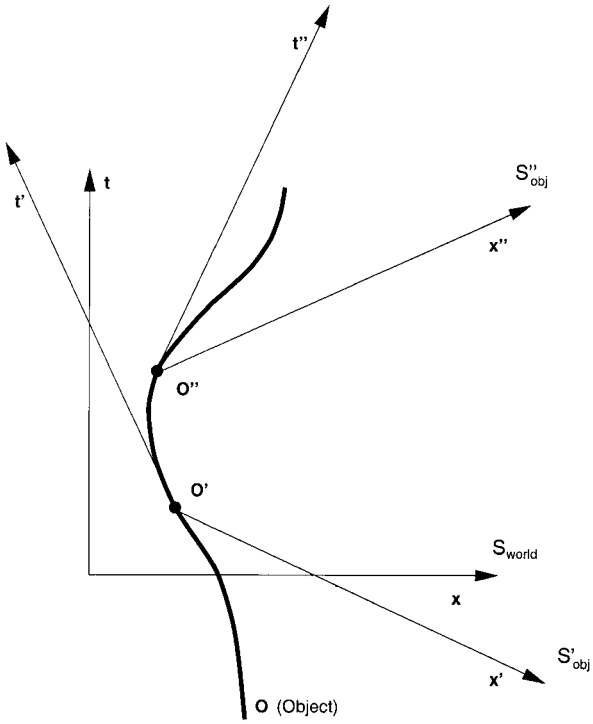

Figure 9. Minkowski diagram showing the trajectory of an accelerated object O within the inertial frame of the outside world, S_{world}. Two examples of co-moving inertial frames of reference are included. These are S'_{obj} and S''_{obj} and they correspond to the points O′ and O″ of the trajectory respectively.

tion this system can be solved, which results in the trajectory of the accelerating object.

References

1. Betts C. Fast rendering of relativistic objects. *The Journal of Visualization and Computer Animation* 1998; **9**: 17–31.
2. Lampa A. Wie erscheint nach der Relativitätstheorie ein bewegter Stab einem ruhenden Beobachter? *Zeitschrift für Physik* 1924; **27**: 138–148.
3. Penrose R. The apparent shape of a relativistically moving sphere. *Proceedings of the Cambridge Philosophical Society* 1959; **55**: 137–139.
4. Terrell J. Invisibility of the Lorentz contraction. *Physical Review* 1959; **116**: 1041–1045.
5. Weisskopf VF. The visual appearance of rapidly moving objects. *Physics Today* 1960; **13**(9): 24–27.
6. Boas ML. Apparent shape of large objects at relativistic speeds. *American Journal of Physics* 1961; **29**: 283–286.
7. Scott GD, Viner RR. The geometrical appearance of large objects moving at relativistic speeds. *American Journal of Physics* 1965; **33**: 534
8. Scott GD, van Driel HJ. Geometrical appearances at relativistic speeds. *American Journal of Physics* 1970; **38**: 971–977.
9. Hsiung PK, Dunn RHP. Visualizing relativistic effects in spacetime. *Proceedings of Supercomputing '89 Conference* 1989; 597–606.
10. Hsiung PK, Thibadeau RH. Spacetime visualization of relativistic effects. *Proceedings of the 1990 ACM Eighteenth Annual Computer Science Conference,* Washington, DC, February 1990; 236–243.
11. Hsiung PK, Thibadeau RH, Cox CB, Dunn RHP, Olbrich PA, Wu M. Wide-band relativistic Doppler effect visualization. *Proceedings of the Visualization 90 Conference*, October 1990; 83–92.
12. Hsiung PK, Thibadeau RH, Wu M. T-buffer: fast visualization of relativistic effects in spacetime. *Computer Graphics* 1990; **24**(2): 83–88.
13. Gekelman W, Maggs J, Xu L. Real-time relativity. *Computers in Physics* 1991; **5**: 372–385.
14. Rau RT, Weiskopf D, Ruder H. Special relativity in virtual reality. In *Mathematical Visualization*, Hege HC, Polthier K (eds). Springer: Heidelberg, 1998; 269–279.
15. Weiskopf D. An immersive virtual environment for special relativity. *Report 108, SFB 382*, University of Tübingen. [Online]. Available: http://www.uni-tuebingen.de/uni/opx/reports/weiskopf_108.ps.gz [January 1999].
16. Weiskopf D, Kraus U, Ruder H. Searchlight and Doppler effects in the visualization of special relativity: a corrected derivation of the transformation of radiance. *ACM Transactions on Graphics* 1999; **18**(3): 278–292.
17. D' Inverno RA. *Introducing Einstein's Relativity*. Clarendon: Oxford, 1992.
18. Misner CW, Thorne KS, Wheeler JA. *Gravitation*. WH Freeman: New York, 1973.
19. Møller C. *The Theory of Relativity* (2nd edn). Clarendon: Oxford, 1972.
20. Rindler W. *Introduction to Special Relativity* (2nd edn). Clarendon: Oxford, 1991.
21. McKinley JM. Relativistic transformations of light power. *American Journal of Physics* 1979; **47**: 602–605.
22. Glassner AS. How to derive a spectrum from an RGB-triplet. *IEEE Computer Graphics and Applications* 1989; **9**(4): 95–99.
23. Judd DB, Wyszecki G. *Color in Business, Science, and Industry* (3rd edn). Wiley: New York, 1975.
24. Wyszecki G, Stiles WS. *Color Science* (2nd edn). Wiley: New York, 1982.
25. Lighthill MJ. *Introduction to Fourier Analysis and Generalised Functions*. Cambridge University Press: Cambridge, 1959.
26. Jackson JD. *Classical Electrodynamics* (3rd edn). Wiley: New York, 1998.
27. Stone MC, Cowan WB, Beatty JC. Color gamut mapping and the printing of digital color images. *ACM Transactions on Graphics* 1988; **7**: 249–292.
28. Hall R. *Illumination and Color in Computer Generated Imagery*. Springer: New York, 1988.
29. Glassner AS. *Principles of Digital Image Synthesis*. Morgan Kaufman: San Francisco, CA, 1995.

30. Hall R, Greenberg DP. A testbed for realistic image synthesis. *IEEE Computer Graphics and Applications* 1983; **3**(8): 10–20.
31. Sun Y, Fracchia FD, Calvert TW, Drew MS. Deriving spectra from colors and rendering light interference. *IEEE Computer Graphics and Applications* 1999; **19**(4): 61–67.
32. Peercy MS. Linear color representations for full spectral sampling. *SIGGRAPH 93 Conference Proceedings*, August 1993; 191–198.
33. Chang MC, Lai F, Chen WC. Image shading taking into account relativistic effects. *ACM Transactions on Graphics* 1996; **15**: 265–300.
34. Hsiung PK, Thibadeau RH, Cox CB, Dunn RHP. Doppler color shift in relativistic image synthesis. *Proceedings of the International Conference on Information Technology*, Tokyo, October 1990; 369–377.

Authors' biographies:

Daniel Weiskopf is a Research Assistant and PhD student in the Department of Theoretical Astrophysics at the University of Tübingen. His research interests include visualization, virtual environments, special and general relativity and quantum field theory. He received an MS in physics from the University of Tübingen.

Ute Kraus works in the Department of Theoretical Astrophysics at the University of Tübingen. Her research interests include visualization, hydrodynamics and X-ray pulsars.

Hanns Ruder is Full Professor of Theoretical Astrophysics at the University of Tübingen. His main research interests are visualization, cataclysmic variables, X-ray pulsars, hydrodynamics, general relativity, biomechanics and atoms in strong magnetic fields. He is a member of the board of management of Astronomische Gesellschaft and is the chairperson of Sonderforschungsbereich (collaborative research project) 382. He received a PhD from the University of Erlangen in 1967.